Geocarto International

ISSN: (Print) (Online) Journal homepage: https://www.tandfonline.com/loi/tgei20

Understanding the influence of land cover change and landscape pattern change on evapotranspiration variations in Gwayi catchment of Zimbabwe

Onalenna Gwate, Hlengiwe Dube, Mbulisi Sibanda, Timothy Dube, Bright Chisadza & Ben Nyikadzino

To cite this article: Onalenna Gwate, Hlengiwe Dube, Mbulisi Sibanda, Timothy Dube, Bright Chisadza & Ben Nyikadzino (2022) Understanding the influence of land cover change and landscape pattern change on evapotranspiration variations in Gwayi catchment of Zimbabwe, Geocarto International, 37:25, 10016-10032, DOI: 10.1080/10106049.2022.2032386

To link to this article: https://doi.org/10.1080/10106049.2022.2032386

GEOCARTO INTERNATIONAL
2022, VOL. 37, NO. 25, 10016–10032
https://doi.org/10.1080/10106049.2022.2032386

Taylor & Francis
Taylor & Francis Group

Check for updates

Understanding the influence of land cover change and landscape pattern change on evapotranspiration variations in Gwayi catchment of Zimbabwe

Onalenna Gwate[a], Hlengiwe Dube[a], Mbulisi Sibanda[b], Timothy Dube[c], Bright Chisadza[a] and Ben Nyikadzino[d]

[a]Department of Geography and Geo-Information Sciences, Lupane State University, Bulawayo, Zimbabwe; [b]Department of Geography, Environmental Studies and Tourism, University of Western Cape, Cape Town, South Africa; [c]Faculty of Natural Sciences, Department of Earth Sciences, Institute of Water Studies,, University of Western Cape, Cape Town, South Africa; [d]Umzingwane Catchment, Zimbabwe National Water Authority, Causeway, Zimbabwe

ABSTRACT
Understanding dynamics in hydrological processes helps to improve water resource management. Climate and land cover changes influence ecohydrological processes. This study sought to assess the influence of climate, land cover and landscape structure dynamics on actual evapotranspiration (ETa). To achieve this, the catchment parameter (*w*) was parameterised and the relationship between ETa and selected landscape metrics was determined. The ratio of precipitation to potential evapotranspiration was < 1 and the w was < 2, suggesting that land cover changes were more influential to ETa changes than climate variations. Given the low w ($1 < w < 2$), we conclude that the catchment had a low water retention capacity and was sensitive to land cover changes. There was a negative correlation between landscape fragmentation and ETa, indicating that unregulated landscape fragmentation could be adversely impacting catchment water balance. Therefore, promoting initiatives that improve land cover consolidation could enhance water retention capacity.

ARTICLE HISTORY
Received 26 May 2021
Accepted 17 January 2022

KEYWORDS
Ecohydrology; catchment parameter; environmental change; water balance; Zimbabwe

1. Introduction

Global environmental change is increasingly shaping the earth and stretching it towards planetary boundaries. For example, land cover change impacts various environmental parameters such as temperature, habitat quality, CO_2 emissions and hydrological processes (Ullah et al. 2019; de Oliveira et al. 2021; Hong et al. 2021; Yohannes et al. 2021a). Climate change and land cover change represent forces that adversely affect the water cycle, water security, water quantity and quality (Jung et al. 2013; Guo et al. 2017; Yu et al. 2020). Land cover change is driven by an increase in pressure on production resources, policy interventions, increasing vulnerability and dynamics in social organization

CONTACT Onalenna Gwate onalennag37@gmail.com
Supplemental data for this article is available online at https://doi.org/10.1080/10106049.2022.2032386.

(Lambin et al. 2003). In southern African countries, the land policies seem to have enhanced land cover changes, which in turn transformed the ecohydrological processes. For instance, the Zimbabwean fast track land reform from the year 2000 resulted in significant land cover changes (Matavire et al. 2015; Jombo et al. 2017). The fast track land reform was characterised by inadequate planning and lack of requisite resources for resettlement. It entailed compulsory acquisition of land from large scale commercial farmers and redistributing to the landless communities in order to address colonial imbalances. Meanwhile, climate change affects the total amount of precipitation received and its partitioning into various components such as evapotranspiration (ET) and runoff (Mao et al. 2015). It is now well established that the global water cycle is gradually changing with terrestrial actual ET (ETa) being the most notable component (Mao et al. 2015). These changes have led to more extreme events such as drought (Shiru et al. 2020) or high precipitation, which society may not be able to cope with (Fisher et al. 2017). Meanwhile, ETa is the biggest flux of the hydrological cycle after precipitation and returns to the atmosphere up to 90% of precipitation in semi-arid environments (Yu et al. 2020). Hence, it is critical to understand ETa variations in the context of global environmental changes related to land cover and climate change.

To gain an improved understanding of the influence of land cover and climate change on catchment hydrology, a number of approaches have been applied. For example, some studies have used paired catchment approaches (Bosch and Hewlett 1982). However, such approaches have not been successful in evaluating the influence of both climate change and land cover change on the hydrological elements (Zhou et al. 2015). The paired catchment experiments seek to demonstrate the impact of land cover change but fail to account for other processes such as climate change. Separating the influences of climate change and land cover change on the hydrological cycle is a daunting task. However, a number of studies have attempted this through the application of the double mass curve or through exploring changes in ETa and trends in land cover change (Chen et al. 2015; Li et al. 2017). In a context of hydrological data paucity in countries such as Zimbabwe, these methods could be untenable and hence, there is need for approaches that simultaneously determine the roles of climate and anthropogenic activities on ETa, using very little observed data such as the Fuh model (Zhou et al. 2015). The Fuh model is a variant of the classical Budyko framework (Budyko 1974) and it uses a single parameter to represent catchment characteristics related to land cover (Chen et al. 2015).

Many studies have described the impact of land cover on ETa, albeit, with different results (Zhang et al. 2017). Generally, it has been recognised that the reduction in forest cover leads to changes in catchment hydrology (Gumindoga et al. 2018; Gwate et al. 2018). Reduction of forest cover tends to result in an increase in runoff and reduction in ETa (Yang et al. 2014; Gwate et al. 2015; Gumindoga et al. 2018; Wang et al. 2021). However, for large catchments, there is uncertainty on catchment response (Zhou et al. 2015). Therefore, there is need to assess catchment responses in Zimbabwe within the purview of environmental changes.

Related to land cover change, landscape pattern structure is also critical in partitioning precipitation into runoff and ETa. The landscape structure is a function of its composition and configuration (McGarigal 1994). Landscape structure is critical in determining the extent of fragmentation in a given landscape. Few studies have explored the impact of landscape structure on hydrological fluxes. For example, Yu et al. (2020) demonstrated that landscape structure plays a critical role in ETa variations in China.

Meanwhile, the ratio of ETa to precipitation (P) or evaporative index is critical since water not discharged in ETa can play an important role in runoff or groundwater recharge. Shifts in ETa/P ratio and other ecohydrological variables have been attributed to changes in vegetation cover (Glenn et al. 2015). This is confirmed by the theoretical framework proposed by Zhang et al. (2001), which showed that the evaporative index of deep rooted woody vegetation was higher than shallow rooted vegetation. However, Huxman et al. (2005) had reservations to this model in some semi-arid environments. The evaporative index could be a useful stable measure of determining the influence of land cover changes on ETa outside areas of monsoon rainfall. For example, Glenn et al. (2015) and Gwate et al. (2018) successfully used the evaporative index to illustrate the impact of land cover change on ETa.

In a context of hydrological data paucity, remotely sensed data is an alternative source of information on land cover dynamics, precipitation, landscape composition and structure. Remotely sensed data are useful in heterogeneous landscapes because they provide detailed spatially explicit information as opposed to point samples, thus representing the whole landscape and its variability. For instance, data sets such as Moderate Resolution Spetroradiometer evapotranspiration (MOD16 ET) (Mu et al. 2011) and the Tropical Applications of Meteorology Using Satellite Data and Ground-Based Observations (TAMSAT) rainfall (Maidment et al. 2014, 2017; Tarnavsky et al. 2014) have been widely used in evaluating catchment hydrological processes (Liaqat and Choi 2017; Gumindoga et al. 2018; Lunyolo et al. 2021). For example, Liaqat and Choi (2017) reported good agreement between observed and modelled (MOD16 ET and Surface Energy Balance System (SEBS)) ETa in different land cover types. These studies illustrate the robustness and suitability of these datasets in understanding ETa. Although a number of studies have been conducted in Zimbabwe to link catchment response to land cover change (for example, Gumindoga et al. 2018), the sizes of such catchments were smaller. Hence, there is need to evaluate the utility of MOD16 ET and TAMSAT datasets in estimating ETa across various land cover types in larger catchments, characterised by high spatial data scarcity. This study sought to determine the influence of land cover, climate and landscape structure changes on ETa in the Gwayi catchment of Zimbabwe. The Gwayi catchment is ungauged and could have been transformed by human activities especially after the fast track land reform in 2000 (Gwate 2012). This study hypothesised that the recent land redistribution of Zimbabwe led to dramatic land cover changes, which impacted on the catchment hydrology. The novelty of this work lies in parameterising the catchment parameter in the study area and multi-source data integration, which can help in estimating impacts of land cover change on hydrological fluxes for catchments that have characteristics similar to the study area.

2. Materials and methods

2.1. Study site

Zimbabwe is divided into seven catchment management areas to facilitate integrated water resources management. The Gwayi catchment consists of five sub-catchments, with total area of 94 858 km^2 (Figure 1). The altitude of the Gwayi catchment varies from 600 m to 1500 m amsl. Mean annual temperature for Gwayi catchment varies from 8.5 to 35° C. Rainfall occurs during the months of October to March (mean monthly rainfall ranging from $\sim 20-180$ mm) and peak flows are experienced during this period. Long term mean catchment rainfall was 650 mm but we found that TAMSAT mean annual rainfall between 2002 and 2019 was 736 mm. The main socio-economic activities in the catchment include rainfed agriculture, cattle and game ranching and fisheries. The catchment was

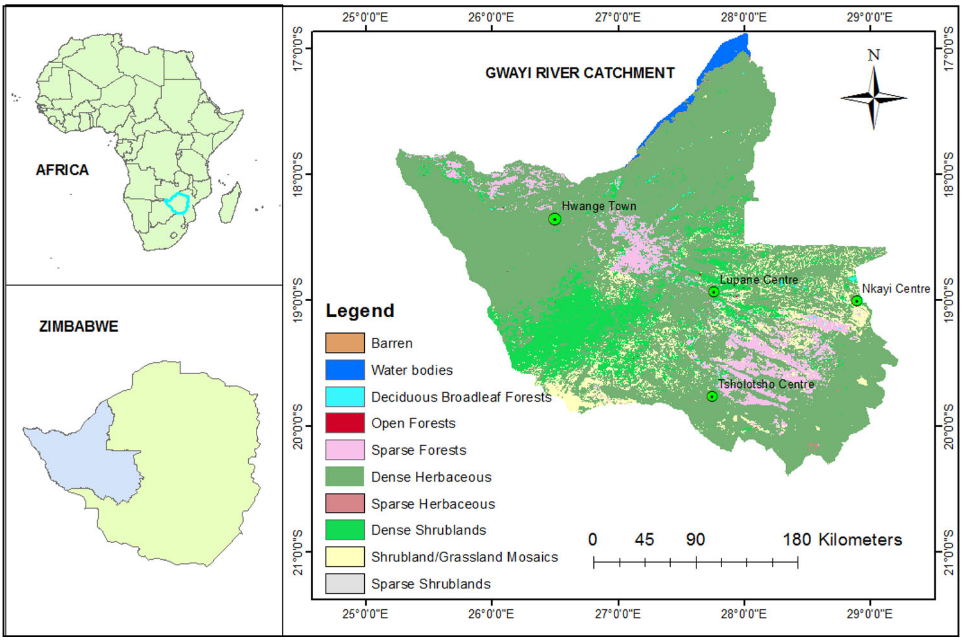

Figure 1. Location of Gwayi catchment showing 2019 land cover types.

not spared from land fragmentation under the auspices of government's fast track land reform programme since the year 2000 and there are a number of land conflicts in the catchment (Ministry of Agriculture, Goz *pers* communication).

2.2. Methods

2.2.1. Datasets

2.2.1.1. Land cover data. The Moderate Resolution Imaging Spectroradiometer land cover (Strahler et al. 1999) product (MCD12Q1), FAO-Land Cover Classification System 1 (LCCS1) land cover layers (https://lpdaac.usgs.gov) were downloaded and used in this study. This is an annual land cover project with a spatial resolution of 500 m. We selected the LCCS1 because it captures the landscape composition and structural variability through many classes that were pertinent to the study area and is standardised globally (http://www.fao.org/3/x0596e/x0596e00.htm). The land covers for Gwayi catchment from 2002 to 2019, were then extracted and are presented (Supplementary material Table 1, Table S1). Given our long study period, years showing watershed changes in land cover type were presented.

2.2.1.2. Evapotranspiration data. The annual potential evapotranspiration (PET) and ETa (Mu et al. 2011) data (MOD16A3 ET) version 6 (v006) acquired in 2002 to 2019 at a spatial resolution of 500 m were download (https://lpdaac.usgs.gov/products/mod16a3v006/) and used in the study to understand ETa variations. This MOD16 ET Collection 6 data product were quality controlled and gap filled by the science team (Running et al. 2017, 2019) following the method proposed by Zhao et al. (2005). Despite this, we also used the extract by attributes tool in Arcmap 10.3.1 to filter out and exclude pixels that were outside the valid range from analysis. Subsequently, the study extracted catchment scale ETa and PET. In addition, we extracted specific land cover type annual ETa for the study period.

2.2.1.3. Rainfall data. TAMSAT datasets were downloaded (http://tamsat.org.uk/view/estimates/index.cgi/rainfall/) and used to determine rainfall within the study area. TAMSAT data has a spatial resolution of 0.0375 degrees (~4 km) and a temporal resolution of 5, 10-day, monthly, and seasonal i.e., Dec-Feb, Mar-May, Jun-Aug, Sep-Nov (Maidment et al. 2014, 2017; Tarnavsky et al. 2014). In this study, we downloaded and used the monthly data from 2002 to 2019. More details on TAMSAT data products are furnished in literature (Maidment et al. 2014, 2017; Tarnavsky et al. 2014).

2.2.2. Data analysis

2.2.2.1. Land cover changes and transfer. We calculated the dynamic degree of single land cover/land use change rate index (K), which describes change in use of a specific land type at the study area for a particular time period following Yang et al. (2017) and Zhao et al. (2020):

$$K = (U_b - U_a)/U_a \times \frac{1}{T} \times 100\%, \qquad [1]$$

where U_a and U_b are areas of land cover/use for a particular land type at the beginning and the end of the time period, respectively; and T is the length of the time period (years). K represents the annual rate of relative change in land cover/use. Note that a positive K indicates an increasing trend for this particular land type whereas a negative K suggests a decreasing trend.

2.2.2.2. Landscape pattern changes analysis. Landscape metrics related to landscape composition and configuration were calculated in Fragstats v4.2.1.603 (McGarigal 1994) at class and landscape levels. Landscape metrics at both class and landscape level were subjected to principal components analysis to reduce data dimensionality and multi-collinearity (Cushman et al. 2008). At the landscape level, the first three components (largest patch index, LPI, edge density (ED) and Shannon diversity index (SHDI)) explained 99.2% of variation while at class level the percentage land (PLAND), ED and LPI accounted for 98.5% of variation. Consequently, we eliminated other metrics such as patch radius of gyration, fractal dimension, total edge, and contiguity index from further analysis (Table S2).

2.2.2.3. Validation of rainfall data. Prior to using TAMSAT data, we converted it from the netCDF format to TIFF images and subsequently extracted the study area. We used the bilinear technique to resample TAMSAT data to 500 m resolution to match other datasets since rainfall data is continuous. Then, we summed up monthly rainfall to get the annual total. The TAMSAT rainfall was validated using observed data from the Zimbabwe National Water Authority at Middle Manyame Catchment (recorded between 2010 and 2018) in Zimbabwe. Subsequently, we applied the root mean square error (RMSE) to evaluate the accuracy of the data.

2.2.2.4. MOD16A3ET data validation with water balance derived ET. There is paucity of observed hydrological data in Zimbabwe and consequently, a shortened water balance equation was used to derive observed catchment ETa. Since the change in storage is negligible on an annual basis (Everson 2001), the water balance equation can be presented as:

$$P - ETa = R \quad [2]$$

where, R is mean annual runoff and all terms have been defined. We obtained observed rainfall and runoff data (2010 – 2018) from Middle Manyame catchment in Zimbabwe. We then applied equation 2 to derive catchment ETa, which was then used to evaluate the accuracy of MOD16A3 ET using the RMSE.

2.2.2.5. Application of the method of cumulative residuals of ETa data. The study assumed strong coupling between changes in catchment scale ETa and dynamics in land cover change (Glenn et al. 2015). Consequently, we applied the method of cumulative residuals (Allen et al. 1998; Costa and Soares 2009; Gwate et al. 2018) to detect changes in catchment ETa.

2.2.2.6. Detecting changes in evapotranspiration and rainfall data. Annual precipitation and annual ETa data were subjected to Mann-Kendall test (Kendall 1938) and Pettitt test (Pettitt 1979) to detect the presence of trends and step changes in the datasets. Similar tests were also conducted to establish the pattern of ETa for each land cover type. Changes in precipitation and ETa could potentially be indicative of fundamental changes in the catchment characteristics linked to climate or land cover dynamics. The non-parametric Mann-Kendall test is commonly employed to detect monotonic trends in series of environmental data, climate data or hydrological data. The null hypothesis (H_0) is that data come from a population with independent realizations and are identically distributed (Pohlert 2020). Autocorrelation and partial autocorrelation were assessed prior to the application of the trend test by examining autocorrelation and partial autocorrelation plots produced from R-3.1.3 software. In all our datasets neither autocorrelation nor partial autocorrelation was detected and the trend test was subsequently applied as is, without the need for correction.

2.2.2.7. Catchment and land cover type based evaporative index. Using the zonal tool in Arcmap 10.3.1, the mean annual ETa from the MOD16A3 ET (v006) product for the whole catchment and for each land cover type were extracted for the period 2002 to 2019. In order to link ETa to land cover change, the evaporative index (ETa/P) for each year was prepared. The extracted ETa was used with TAMSAT rainfall to calculate the evaporative index for the entire catchment and for each land cover type. The evaporative index is a stable measure that illustrates partitioning of precipitation and any marked changes could be indicative of changes in catchment characteristics related to land cover change.

2.2.2.8. Determining catchment parameter. Owing to paucity of observed data, the study applied the Fuh model, published in Chinese in 1981 (Zhang et al. 2004) to detect the influence of land cover change and climate factors on ETa:

$$ET/P = 1 + PET/P - \left[1 + (PET/P)^w\right]^{1/w} \quad [3]$$

where w is a model parameter varying from 1 to infinity and indicates the integrated catchment characteristics such as vegetation cover, soil properties and slope, PET is potential evapotranspiration, which is a proxy for net radiation (Wang et al. 2016) and P is precipitation.

The catchment parameter (w) was estimated using optimization by fitting equation (3) to ETa from the MOD16A3 ET product and annual TAMSAT rainfall (2002–2019) using the *rgenoud* package (Mebane and Sekhon 2011; 2019) in R-3.1.3 software. The optimization sought to minimise the difference between ETa derived from the shortened water balance equation (equation 2) and MOD16A3 ET (v006) for each year. The catchment parameter (w) is a proxy for integrated catchment characteristics largely linked to land cover (Roderick and Farquhar 2011; Li et al. 2013; Chen et al. 2015; Zhou et al. 2015). Subsequently, the study tested the catchment parameter for step change (Pettitt's test) and existence of a trend (Mann-Kendall test) over the years (2002–2019). Equation (3) has successfully been used to evaluate the impacts of land cover and climate change on hydrological fluxes (Zhang et al. 2004; Chen et al. 2015; Zhou et al. 2015; Gwate et al. 2018). Zhou et al. (2015) identified two critical values at P/PET $= 1$ and $w > 2$, which help to decipher catchment hydrological response. P/PET plays a more important role than w when $w > 2$, and less when $w < 2$. Hence, equation 3 can be used for evaluating impacts of both land cover and climate change on catchment hydrological response. There is need to parameterise w in the context of Zimbabwe for an improved comparative understanding of the impacts of climate and land cover change on hydrological response.

2.2.2.9. Determining the influence of land cover change and landscape pattern on ETa. Linking dynamics in evapotranspiration to land cover and landscape pattern change is a daunting task. We applied the evaporative index, catchment parameter (w) from equation 3 and correlation analysis to decipher the link between ETa changes to land cover and landscape pattern changes.

3. Results

3.1. Land cover change at gwayi river catchment

The cumulative residuals of MOD16A3 ET showed inflection points in 2013 and 2016 (Supplementary material Figure 1, Figure S1). Subsequently, the 2002, 2013 and 2016 images were used to represent years of watershed land cover changes. The year 2000 and 2001 images were not available for the study site.

The total land area of Gwayi catchment was 98 858 km^2 with nine land cover types and the 2019 land cover distribution is presented (Figure 1). Dense herbaceous cover accounted for 73% of the catchment and was evenly distributed throughout the catchment while Deciduous Broadleaf Forests were mainly located to the east of the catchment in Nkayi district. Dense shrublands were mainly found in the southwest in Tsholotsho district. Grasslands were also found in the southwest and the eastern part of the catchment. The Sparse forests comprised of a narrow belt that stretched diagonally from the north-western tip of the catchment to the upper south-eastern part (Figure 1). Sparse forests were found mainly adjacent to Shrubland/Grassland mosaics and Dense Shrublands cover types. Barren and water bodies land cover types were mainly concentrated in the northern edge of the catchment. Dynamics in land cover changes are presented (Table 1).

3.2. Trends in land cover change

During the years 2002 – 2013 and 2016 – 2019 most of land cover types had a negative trend/degree of land cover change whilst during 2013 – 2016 most land cover types showed a positive rate of change (Table 2).

Table 1. Land cover changes 2002 – 2019.

Land cover type	Area (km^2) 2002	2013	2016	2019
Barren	51.25	58.25	75.50	72.00
Water bodies	1149.00	1140.50	1085.00	1099.75
Deciduous Broadleaf Forests	28.75	120.50	145.25	131.50
Open Forests	738.50	371.25	822.50	33.50
Sparse Forests	5402.75	9137	8215.50	7385.00
Dense Herbaceous	68841.75	67480	67524.00	66997.00
Sparse Herbaceous	110.25	86.25	85.75	73.50
Dense Shrublands	16206.25	12662.25	12476.00	11906.75
Shrubland/Grassland Mosaics	2321.75	3798.75	4421.50	7152.25
Sparse Shrublands	7.50	3.25	7.00	6.75
Total	94858	94858	94858	94858

Table 2. Rate of land cover change (%) during the study period (2002 – 2019).

Land cover type	2002 – 2013 (%)	2013– 2016 (%)	2016 – 2019 (%)	2002 – 2019 (%)
Barren	1.14	7.40	−1.16	2.38
Water bodies	−0.06	−1.22	0.34	−0.25
Deciduous Broadleaf Forests	26.59	5.13	−2.37	21.02
Open Forests	−4.14	30.39	−23.98	−5.62
Sparse Forests	5.76	−2.52	−2.53	2.16
Dense Herbaceous	−0.16	0.02	−0.20	−0.16
Sparse Herbaceous	−1.81	−0.14	−3.57	−1.96
Dense Shrublands	−1.82	−0.37	−1.14	−1.56
Shrubland/Grassland Mosaics	5.30	4.10	15.44	12.24
Sparse Shrublands	−4.72	28.85	−0.89	−0.59

Table 3. Average landscape metrics for selected land cover types (2002 – 2019).

Landscape metric*	Barren	Deciduous Broadleaf Forests	Open Forests	Sparse Forest	Dense Herbaceous	Sparse Herbaceous	Dense Shrublands	Shrubland /Grassland Mosaics	Sparse Shrublands
PLAND (%)	0.06	0.01 2	0.383	7.822	71.181	0.101	15.033	3.955	0.005
LPI (%)	0.015	0.003	0.064	1.827	69.042	0.009	6.867	0.977	0.001
ED (m ha^{-1})	4762.312	596.459	16067.511	177554.178	525502.593	6416.794	367687.754	165009.111	392.554

*From Table 3, PLAND - Percentage of landscape, LPI - Largest Patch Index and ED – Edge density

3.3. Dynamics in landscape pattern

The long-term term average landscape metrics for selected land cover types examined in this study are presented (Table 3). At the landscape level, we found a trend ($p < 0.01$) in the SHDI (tau = 0.60) and ED (tau = 0.83) while neither a trend nor a step change could be found in LPI (tau) = −0.25). With respect to class level (Table 4), most metrics revealed a trend ($p < 0.05$) except for Sparse Shrublands where a step change ($p < 0.05$) was detected in the LPI metric and the year of inflection was 2009. Neither trends nor step changes were observed in the land metrics for Barren, Deciduous Broadleaf Forests and Open Forest but Kendall's tau was instructive on trajectories (Table 4). At both landscape and class level, the correlation between land metrics and ETa was weak ($p > 0.05$).

3.4. Pattern of catchment evapotranspiration and rainfall

Results revealed that MOD16A3 ET was similar to observed ETa (RMSE = 32 mm or 5%) per year when the observed annual mean ETa was 649 mm in the Middle Manyame catchment (N = 9). On the other hand, TAMSAT rainfall had a RMSE of 116 mm (N = 9)

Table 4. Mann-Kindall's tau for land metrics per land cover type (2002 – 2019) *$p < 0.05$.

Landscape metric*	barren	Deciduous Broadleaf Forests	Open Forests	Sparse Forest	Dense Herbaceous	Sparse Herbaceous	Dense Shrublands	Shrubland/ Grassland Mosaics	Sparse Shrublands
PLAND (%)	0.20	0.20	−0.25	0.56*	0.32	0.32	−0.75*	0.75*	−0.22
LPI (%)	0.33	0.18	−0.16	0.16	−0.25	−0.25	−0.51**	−0.51*	−0.20
ED (m ha^{-1})	0.28	0.18	−0.26	0.65	0.81*	0.813*	−0.84*	−0.84*	−0.21

*From Table 4, PLAND - Percentage of landscape, LPI - Largest Patch Index and ED – Edge density

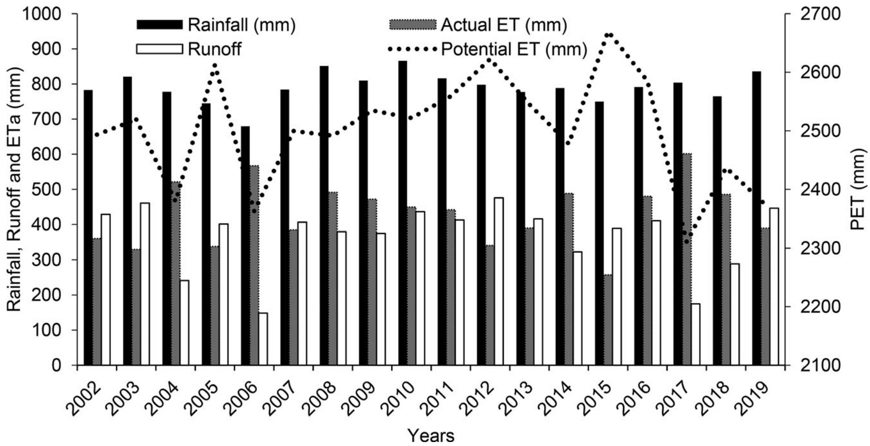

Figure 2. Pattern of rainfall, actual evapotranspiration (ETa) and potential evaporation (PET).

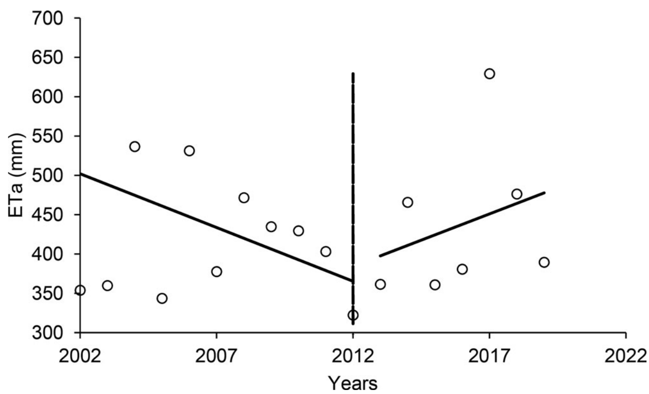

Figure 3. Pattern of actual evapotransportation (ETa) of Gwayi catchment (2002 – 2019).

per annum (16%) when mean observed annual rainfall was 736 mm. Long term average evapotranspiration, rainfall, evaporative index, ratio of runoff to precipitation (R/P), P/PET and ET/PET for Gwayi catchment are presented (Table S3).

The difference between PET and ETa was high (Figure 2). Based on the shortened water balance equation, estimated mean annual runoff over the study period was 343 mm, with an annual rate of change of 5.6 mm. Runoff exceeded ETa in 2002, 2003, 2005, 2007, 2012, 2013, 2015 and 2019.

We detected a break in ETa data around the year 2012 (Figure 3). Hitherto, mean annual ETa was decreasing at a rate of 14 mm $year^{-1}$. From 2013 to 2019, ETa was increasing at a rate of 13 mm $year^{-1}$. During the whole study period, ETa was declining at an annual rate of

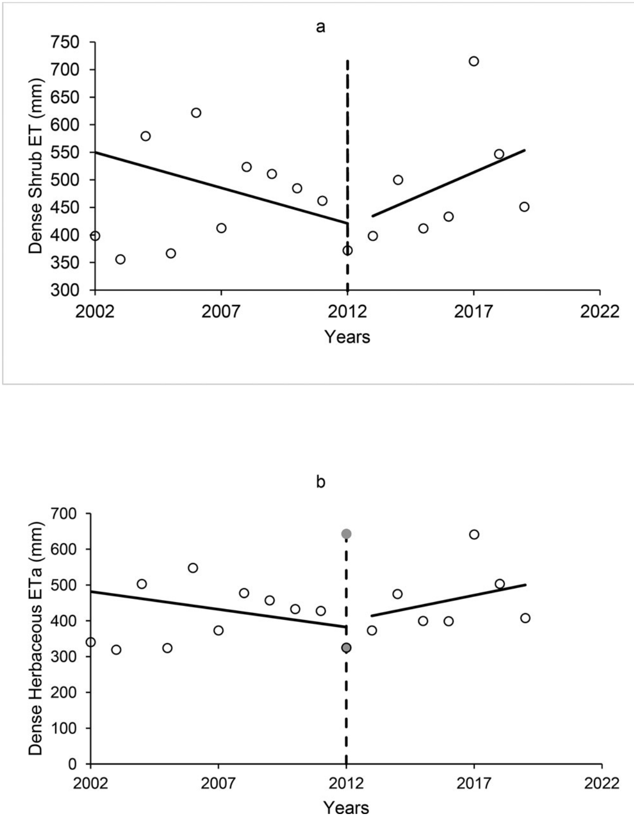

Figure 4. Dynamics in evapotranspiration of a) Dense Shrubland and b) Dense Herbaceous, land cover types (2002 – 2019).

3.5 mm. However, neither a trend nor a step change was detected in rainfall and PET data but the Mann-Kendall's tau (0.18) and (0.20) respectively, suggest increasing patterns.

3.4.1. Average land cover based ET

Despite relatively low spatial coverage, Barren (< 0.1%), Deciduous Broadleaf forests (< 0.2%) and Sparse Shrublands (< 0.01%) contributed relatively high ETa over the study period (Table S4). Barren land cover type had the least evaporative index while Deciduous Broadleaf Forests cover type had the highest (Table S4).

Step changes in ETa were noted in Dense Shrub and Dense Herbaceous (Figure 4) land cover types. A statistically significant upward trend ($p < 0.05$, Kendall's tau $= 0.37$) was observed for Sparse Herbaceous and Sparse Shrublands ($p < 0.05$, tau $= 0.35$) land cover types respectively. On the other hand a downward trend for Barren ($p < 0.05$, tau $= -0.35$) was detected while neither trends nor step changes were detected for open forests (tau $=$ 0.02), Deciduous Broadleaf Forests (tau $= -0.09$), Sparse forests (tau $= -0.01$) and Shrubland/ Grassland Mosaics (tau $= 0.03$) land cover types.

3.5. Influence of land cover change on ETa

3.5.1. Evapotrative index of selected land cover type

Average evaporative index for selected land cover types in specific years is shown in Figure S2. Significant downward trends ($p < 0.05$) in the evaporative index of Barren land

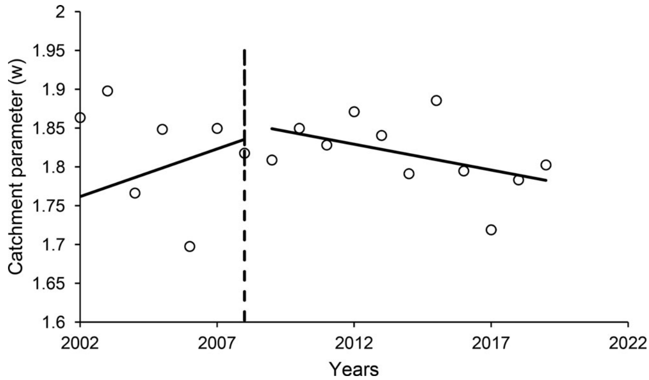

Figure 5. Dynamics in the catchment parameter (*w*) during the study period (2002 – 2019).

cover (tau = −0.36), Sparse shrubland (tau = −0.38) and Sparse Herbaceous (tau = −0.36) were observed during the study period. Deciduous broadleaf forest (tau = 0.2), Open forest and Sparse Forests (tau = 0.04), Dense Herbaceous shrubland (tau = 0.02), Shrubland/Grassland (tau = 0.03) and Dense shrubland (tau = 0.02) displayed marginal increasing patterns in evaporative index

3.5.2. Pattern of catchment parameter

The w values ranged from 1.64 to 1.90 with an average of 1.81. A breakpoint in the w data was noted in 2008. The w increased and decreased at an annual rate of 0.01 between 2002 and 2008 and 2009 and 2019 respectively (Figure 5).

3.5.3. Correlation between ETa and landscape pattern

At both landscape and class level, the correlation between land metrics and ETa was weak ($r = -0.45 - 0.12$, $p > 0.05$).

4. Discussion

4.1. Dynamics in land cover change in gwayi catchment

The study sought to understand the influence of land cover change, landscape composition and configuration on ETa. The method of cumulative residual helped to detect watershed ETa changes, which in turn were reflective of magnitudes of land cover changes. Dynamics in the Barren land cover type were largely related to changes in water levels in the Zambezi River at the Zimbabwe – Zambia boundary as most barren pixels were observed along the Kariba dam in the Zambezi River. The flows in the Zambezi were not only influenced by rainfall in Zimbabwe but also rainfall received in upstream countries such as Angola and Zambia. The increasing trend in the Barren land cover type between 2002 and 2016 is indicative of low flows into the Zambezi and the decreasing trend (2016 − 2019) suggests high flows through the Zambezi River. The overall increase in Barren land cover accompanied by an overall decrease in water cover during the study period suggests a general decrease in inflows into the Zambezi river/lake Kariba and this is consistent with a projected drying trend in the Zambezi basin (Hughes and Farinosi 2020). The positive rate of relative change in land cover types such as Deciduous Broadleaf Forests, Sparse Forests and Shrubland/Grassland mosaic could be related to fire exclusion. The pockets of Deciduous Broadleaf Forests and Open forests land cover types were located within the Miombo woodlands and recent efforts to improve the management of Miombos (World Wide Fund for Nature 2012) could have resulted in reduced fire incidents, allowing for the two land cover types to expand. On the other hand increasing Shrubland/Grassland mosaics land cover type could be related to high veld fire incidents in such areas resulting in some trees dying. Although it is well established that woody thickening is taking place in southern Africa owing to CO_2 and N fertilisation (Wigley et al. 2010; O'Connor et al. 2014), we speculate that in Zimbabwe, this pattern is being counteracted by annual burning owing to unplanned veld fires since the watershed 2000 fast track land reform. The rate of relative land cover change was negative for Open Forests, Sparse Herbaceous, Dense Herbaceous and Dense Shrublands, suggesting that these land covers were slightly shrinking due to human activities.

4.2. Rainfall and ETa data quality

The application of remotely sensed data is critical in data scarce areas. In Zimbabwe, there is paucity of water fluxes measurement stations. Hence, the study leveraged on remotely sensed data. The RMSE for ETa was within 5% of ETa derived from the shortened water balance, indicating that MOD16 ET successfully reproduced observed catchment ETa. On the other hand the RMSE for rainfall was 16% of the observed annual mean, indicating relatively good model fit. Therefore, for practical purposes, the TAMSAT rainfall and MOD16ET products were able to simulate observed data with marginal error. Hence, we have confidence in the application of these products in this catchment. The relatively good fit in rainfall and ETa data suggests that the runoff derived from the shortened water balance equation reported in this paper is also accurate. Runoff accounted for 43% of rainfall and this suggests that catchment yield was relatively high in a context where ETa accounted 56% of precipitation. These results suggest that precipitation converted to ETa was below the global average of 60% (Mu et al. 2011) but higher than the average for Africa (16%) reported by Karamage et al. (2018). During some years, runoff exceeded ETa, possibly due to patchy vegetation, high soil antecedent moisture conditions or high rainfall intensity given that convectional rainfall predominates in the catchment (Love et al. 2010). For example, Huxman et al. (2005) and Tang et al. (2021) illustrated that rainfall characteristics, soil and vegetation cover interact in a complex manner to generate runoff.

4.3. Dynamics in catchment ETa

The difference between ETa and PET was consistently high, suggesting that the catchment was water limited and the low wetness index confirmed this. On a catchment scale, a step change was detected in ETa around the year 2012 even though neither a step nor trend was detected in rainfall. The step change in ETa in 2012 could be indicative of broad based land cover changes in the catchment that resulted in hydrological response. The decreasing trajectory in ETa before 2012 is consistent with the negative annual rate of land cover change for most land cover types. Overall, ETa was declining while runoff was increasing, suggesting that the catchment's ability to store water was declining. This decrease in ETa was inconsistent with the reported increase in global ETa owing to human induced increase in woodlands (Wang et al. 2021). Woodlands were declining in the study area and land cover maps confirm this pattern. With respect to individual land cover types, step changes in Dense Herbaceous and Dense Shrublands ETa were reflective of the magnitude of trends in land cover changes. It is well established that changes in land cover type and size affect ETa. For example, Cristina et al. (2015) found that mean annual evapotranspiration was 39% lower in agricultural ecosystems than in natural ecosystems. Consequently, a decrease in spatial coverage of a particular land cover inadvertently translates to a decrease in total ETa from that particular land cover type. For example, land cover types that accounted for over 80% of the total catchment area were contracting up to 2012. The expansion of most land cover types between 2013 and 2016 could have led to an increasing trajectory in ETa of the catchment and this is consistent with results from elsewhere (Yang et al. 2017; Gwate et al. 2018), indicating strong coupling between land cover change and ETa.

4.4. Impact of landscape metrics on ETa

Landscape metrics are reflective of the combination of natural processes and anthropogenic activities in the landscape. Consequently, different landscape types will affect different environmental processes such as the partitioning of precipitation into various components (Zhang et al. 2019). At the landscape scale, we found increasing trends in SHDI and ED, suggesting that the catchment was becoming more heterogeneous/diverse and fragmented. The increasing SHDI and ED were accompanied by decreasing ETa, suggesting that the landscape was undergoing degradation as patches and edge were increasing. Yu et al. (2020) also found that land fragmentation led to a decline in ETa. From a shortened water balance perspective (Everson 2001), declining ETa suggests that runoff could be relatively high or increasing. Results from this paper confirmed that runoff was relatively high and was increasing in this catchment. It is well established that increasing runoff undermines water retention capacity, increases catchment yield and is symptomatic of high soil erosion (Zhou et al. 2015; Yohannes et al. 2021b). Hence, landscape fragmentation in this case could be leading to catchment degradation. This fragmentation could have been caused by settlement under the auspices of the fast track land reform programme (Jombo et al. 2017), leading to an increase in pressure on production resources (Lambin et al. 2003). However, this result was different from Zhang et al. (2019) who reported declining runoff and sediment load in Loess Plateau as a result of fragmentation of agricultural land. The difference in results was due to the fact that the Loess Plateau was under the greening programme that sought to return agricultural lands into forest. Hence, fragmenting large homogenous agricultural lands into new forest landscapes led to a decline in runoff and soil erosion. Therefore, the impact of landscape metrics on hydrological processes varies with the nature of landscape types. In terms of landscape composition at class level, low average PLAND and LPI for Barren, Deciduous Broadleaf Forests, Sparse Herbaceous, Sparse Shrublands, Shrubland/Grassland mosaic was reflective of the low spatial coverage by these classes. However, these land cover types were likely to degrade into other less beneficial classes since results suggest that the entire catchment/landscape was fragmenting. This is further confirmed by high average ED for all classes, indicating a high degree of edge.

4.5. Impacts of land cover change and climate on ETa

Impacts of land cover on ETa were assessed using three parallel lines of evidence. These include the catchment parameter (w), the evaporative index and land cover maps. The influence of the latter on ETa has already been discussed (section 4.3). The w is an integration constant that is dimensionless and independent of P and PET, and represents watershed characteristics. Based on Zhou et al. (2015) theoretical analysis, Gwayi catchment had a low water retention capacity ($1 < w < 2$) because of the prevalence of sparse vegetation in the catchment. On the other hand, high vegetation cover in the catchment could result in $w > 2$ and this would buffer catchment hydrological response. Hence, Gwayi catchment yield was relatively high and this was confirmed by a relatively high runoff, accounting for 43% of precipitation. Catchments with relatively low *w*, ($1 < w < 2$), are sensitive to land cover changes and the *w* plays an important role in determining catchment yield (Zhou et al. 2015; Zhang et al. 2017; Gwate et al. 2018). The sensitivity of Gwayi catchment to water yield was also confirmed by a very low wetness index (P/PET) reported in this study. It is also well established that when the P/PET ratio is > 1, climate factors play a more significant role in catchment response than when $w > 2$ and less when $w < 2$ (Zhou et al. 2015). Therefore, it can be concluded that land cover changes as captured in *w* were more influential in Gwayi catchment hydrological response compared to climatic factors captured in the P/PET ratio. Step changes in total catchment ETa responded to step changes in the *w*, indicating a shift in catchment yield due to changes in vegetation characteristics. The increasing pattern of the *w* up to 2008 suggests that catchment vegetation cover was relatively high compared to the period after 2008 to 2019. The changes in vegetation during this period were related to the first phase of fast track land reform programme (Gwate 2012) that led to land fragmentation, whose effect could have become more pronounced by the year 2008. Hence, after 2008, the *w* was, declining suggesting that vegetation destruction was taking place in the catchment.

Our results also suggest that high evaporative index was associated with vegetation physiognomic type. Land cover types with deep rooted vegetation had relatively higher evaporative index and this was consistent with other studies (Zhang et al. 2001; Gwate et al. 2018). Hence, land cover changes affected the partitioning of precipitation into ETa and runoff. The changes in the evaporative index is reflective of fundamental changes in land cover types (Glenn et al. 2015). However, the relatively higher evaporative index in the Shrubland/Grassland mosaic is indicative of efficient water uptake by a combination of shallow and relatively deep rooted plants in this land cover type. Grass plants were effective in utilising water in the upper layers of the soil while the shrubs utilised water beyond the soil moisture zone.

5. Conclusions

The study sought to determine the influence of land cover and landscape pattern changes on ETa. Changes in ETa that took place in the catchment were largely driven by human activities than climate factors. This was reflected by the *w* and P/PET ratio of the catchment as well as a relatively low water retention capacity. Hence, Gwayi catchment was water limited and the catchment yield is highly sensitive to land cover changes. The catchment was fragmenting resulting in a decreasing trajectory of ETa. Step changes in total catchment ETa responded to step changes in the *w*, indicating a shift in catchment yield due to changes in vegetation characteristics. Vegetation physiognomic types influenced the P/ETa ratio and the ETa was strongly coupled to dynamics in landscape pattern, hence the P/ETa ratio is a useful index for determining land cover and landscape pattern changes. Results of this study are valid since there was good agreement between remotely sensed rainfall and ETa. The application of the *w* approach in this study provided a holistic picture of how both land cover and climate changes influenced water yield as opposed to reliance on paired catchment studies since the latter may not be used to evaluate the influence of climate. In order to improve catchment water retention capacity, it will be necessary to promote schemes that improve landscape/land cover consolidation since fragmentation adversely affected ETa.

Disclosure statement

No potential conflict of interest was reported by the authors.

ORCID

Onalenna Gwate http://orcid.org/0000-0003-0237-4316
Timothy Dube http://orcid.org/0000-0003-3456-8991

References

Allen RG, Pereira LS, Raes D, Smith M. 1998. Crop evapotranspiration (guidelines for computing crop water requirements). FAO Irrigation and Drainage Paper No. 56. Rome: FAO. http://www.kimberly.uidaho.edu/water/fao56/fao56.pdf.

Bosch JM, Hewlett JD. 1982. A review of catchment experiments to determine the effect of vegetation changes on water yield and evapotranspiration. J Hydrol. 55(1–4):3–23.

Budyko MI. 1974. Climate and life. Orlando (FL): Academic Press.

Chen X, Liu X, Zhou G, Han L, Liu W, Liao J. 2015. 50-year evapotranspiration declining and potential causations in subtropical Guangdong province, southern China. Catena. 128:185–194.

Costa AC, Soares A. 2009. Homogenization of climate data: Review and new perspectives using geostatistics. Math Geosci. 41(3):291–305.

Cristina L, Dias P, Macedo MN, Heil M, Coe MT, Neill C. 2015. Effects of land cover change on evapotranspiration and streamflow of small catchments in the Upper Xingu River Basin, Central Brazil. J Hydrol Reg Stud. 4:108–122.

Cushman SA, McGarigal K, Neel MC. 2008. Parsimony in landscape metrics: strength, universality, and consistency. Ecol Indic. 8(5):691–703.

de Oliveira SEA, Tavares SM, Rocha FT, Conceiçao P de AL, Cleber dos S, Maria M d L, Vicente d P d S, Francisco d AS d S, Jose CGD. 2021. Impacts of land use and land cover changes on hydrological processes and sediment yield determined using the SWAT model. Int J Sediment Res. 37(1):54–69.

Everson CS. 2001. The water balance of a first order catchment in the montane grasslands of South Africa. J Hydrol. 241(1–2):110–123.

Fisher JB, Melton F, Middleton E, Hain C, Anderson M, Allen R, Mccabe MF, Hook S, Baldocchi D, Townsend PA, et al. 2017. The future of evapotranspiration: Global requirements for ecosystemfunctioning, carbon and climate feedbacks, agriculturalmanagement, and water resources. Water Resour Res. 53(4):2618–2626. 2618–2626. doi:10.1002/2016WR020175.Received

Glenn EP, Scott RL, Nguyen U, Nagler PL. 2015. Wide-area ratios of evapotranspiration to precipitation in monsoon-dependent semiarid vegetation communities. J Arid Environ. 117:84–95.

Gumindoga W, Rwasoka DT, Ncube N, Kaseke E, Dube T. 2018. Effect of landcover/land-use changes on water availability in and around Ruti Dam in Nyazvidzi catchment, Zimbabwe. Water SA. 44(1):136–145.

Guo D, Westra S, Maier H. 2017. Impact of evapotranspiration process representation on runoff projections from conceptual rainfall-runoff models. Water Resour Res. 53(1):435–454.

Gwate O. 2012. Comparison of community composition in disturbed and relatively undisturbed rangelands in semi arid regions using ground based methods: the case of Insindi commercial farm and Insindi A1 resettlement area, Gwanda, Zimbabwe. J Environ Res Dev. 6:1119–1126.

Gwate O, Mantel SK, Gibson LA, Munch Z, Palmer AR. 2018. Exploring dynamics of evapotranspiration in selected land cover classes in a sub-humid grassland: a case study in quaternary catchment S50E, South Africa. J Arid Environ. 157:66–76.

Gwate O, Woyessa YE, Wiberg D. 2015. Dynamics of land cover and impact on stream flow in the Modder river basin of South Africa : case study of a quaternary catchment. Int J Environ Prot Policy. 3(2):31–38.

Hong C, Burney JA, Pongratz J, Nabel JEMS, Mueller ND, Jackson RB, Davis SJ. 2021. Global and regional drivers of land-use emissions in 1961–2017. Nature. 589(7843):554–580.

Hughes DA, Farinosi F. 2020. Assessing development and climate variability impacts on water resources in the Zambezi River basin. Simulating future scenarios of climate and development. J Hydrol Reg Stud. 32:100763

Huxman TE, Wilcox BP, Breshears DD, Russel LS, Snyder K, Small EE, Hultine K, Pockman WT, Jackson RBJ. 2005. Ecohydrological implications of woody plant encroachment. Ecology. 86(2): 308–319.

Jombo S, Adam E, Odindi J. 2017. Quantification of landscape transformation due to the Fast Track Land Reform Programme (FTLRP) in Zimbabwe using remotely sensed data. Land Use Policy. 68:287–294.

Jung IW, Chang H, Risley J. 2013. Effects of runoff sensitivity and catchment characteristics on regional actual evapotranspiration trends in the conterminous US. Environ Res Lett. 8(4):044002–044007.

Karamage F, Liu Y, Fan X, Justine MF, Wu G, Zhou H, Wang R. 2018. Spatial relationship between precipitation and runoff in Africa. Hydrol Earth Syst Sci Discuss. https://doi.org/10.5194/hess-2018-424.

Kendall AMG. 1938. A New Measure of Rank Correlation. Biometrika Trust. 30(1–2):81–93.

Lambin EF, Geist HJ, Lepers E. 2003. Dynamics of land-use and land-cover change in tropical regions. Annu Rev Environ Resour. 28(1):205–241.

Li D, Pan M, Cong Z, Zhang L, Wood E. 2013. Vegetation control on water and energy balance within the Budyko framework. Water Resour Res. 49(2):969–976.

Li G, Zhang F, Jing Y, Liu Y, Sun G. 2017. Response of evapotranspiration to changes in land use and land cover and climate in China during 2001-2013. Sci Total Environ. 596-597:256–265.

Liaqat UW, Choi M. 2017. Accuracy comparison of remotely sensed evapotranspiration products and their associated water stress footprints under different land cover types in Korean peninsula. J Clean Prod. 155:93–104.

Love D, Uhlenbrook S, Corzo-Perez G, Twomlow S, Van der Zaag P. 2010. Rainfall – interception – evaporation – runoff relationships in a semi-arid catchment, northern Limpopo basin, Zimbabwe. Hydrol Sci J. 55(5):687–703.

Lunyolo LD, Khalifa M, Ribbe L. 2021. Assessing the interaction of land cover/land use dynamics, climate extremes and food systems in Uganda. Sci Total Environ. 753:142549

Maidment RI, Grimes D, Allan PR, Tarnavsky E, Stringer M, Hewison T, Roebeling R, Black E. 2014. The 30 year TAMSAT African rainfall climatology and time series (TARCAT) data set. J Geophys Res Atmos. 119(18):10619–10644.

Maidment RI, Grimes D, Black E, Tarnavsky E, Young M, Greatrex H, Allan RP, Stein T, Nkonde E, Senkunda S, Alcántara EMU. 2017. A new, long-term daily satellite-based rainfall dataset for operational monitoring in Africa. Sci Data. 4:170063.

Mao J, Fu W, Shi X, Ricciuto DM, Fisher JB, Dickinson RE, Wei Y, Shem W, Piao S, Wang K, et al. 2015. Disentangling climatic and anthropogenic controls on global terrestrial evapotranspiration trends. Environ Res Lett. 10(9):094008.

Matavire MM, Sibanda M, Dube T. 2015. Assessing the aftermath of the fast track land reform programme in Zimbabwe on land-use and land-cover changes. Trans R Soc S Afr. 70 (2):181–186.

McGarigal MB. 1994. Fragstats: spatial pattern analysis program for quantifying landscape structure. [accessed 2020 Dec 20]. Available from: https://www.umass.edu.

Mebane AWR, Sekhon JS. 2019. Package 'rgenoud.' [accessed 2021 Feb 22]. Available from: https://cran.r-project.org/web/packages/rgenoud/rgenoud.pdf.

Mebane WRJ, Sekhon JS. 2011. Genetic optimization using derivatives: the rgenoud package for R.. J Stat Software. 42(11):1–26. Available from: http://www.jstatsoft.org/v42/i11.

Mu Q, Zhao M, Running SW. 2011. Improvements to a MODIS global terrestrial evapotranspiration algorithm. Remote Sens Environ. 115(8):1781–1800.

O'Connor TG, Puttick JR, Hoffman MT. 2014. Bush encroachment in Southern Africa: changes and causes. African J Range Forage Sci. 31(2):67–88..

Pettitt AN. 1979. A non-parametric approach to the change-point problem. J R Stat Soc Ser C. 28(2): 126–135.

Pohlert T. 2020. Non-parametric trend tests and change-point detection 1–18. [accessed 2021 Mar 10]. Available from: https://cran.r-project.org.

Roderick ML, Farquhar GD. 2011. A simple framework for relating variations in runoff to variations in climatic conditions and catchment properties. Water Resour Res. 47(12):W00G07.

Running S, Mu Q, Zhao M, Moreno A. 2017. MODIS 16 user's guide MODIS global terrestrial evapotranspiration (ET) product (NASA MOD16A2/A3) NASA earth observing system MODIS land algorithm. [accessed 2020 Mar 30]. Available from: https://ladsweb.modaps.eosdis.nasa.gov/missions-and-measurements/modis/MOD16_ET_User-Guide_2017.pdf.

Running SW, Mu Q, Zhao M, Moreno A. 2019. User's guide MODIS global terrestrial evapotranspiration (ET) product NASA earth observing system MODIS land algorithm (for collection 6). [accessed 2020 Mar 30]. Available from: https://landweb.modaps.eosdis.nasa.gov/QA_www/forPage/user_guide/MOD16UsersGuideV2.2June2019.pdf

Shiru MS, Shahid S, Dewan A, Chung E, Noraliani A, Kamal A, Hassan QK. 2020. Projection of meteorological droughts in Nigeria during growing seasons under climate change scenarios. Sci Rep. 10(1):10107

Strahler A, Gopal S, Lambin E, Moody A. 1999. MODIS land cover product algorithm theoretical basis document (ATBD) MODIS land cover and land-cover change, change. [accessed 2020 Sep 2]. Available from: https://lpdaac.usgs.gov

Tang C, Liu Y, Li Z, Guo L, Xu A, Zhao J. 2021. Effectiveness of vegetation cover pattern on regulating soil erosion and runoff generation in red soil environment, southern China. Ecol Indic. 129:107956.

Tarnavsky E, Grimes D, Maidment R, Black E, Allan RP, Stringer M, Chadwick R, Kayitakire F. 2014. Extension of the TAMSAT satellite-based rainfall monitoring over Africa and from 1983 to present. J Appl Meteorol Climatol. 53(12):2805–2822.

Ullah S, Tahir AA, Akbar TA, Hassan QK, Dewan A, Khan JA, Khan M. 2019. Remote sensing-based quantification of the relationships between land use land cover changes and surface temperature over the Lower Himalayan Region. Sustainability. 11:5492.

Wang C, Wang S, Fu B, Zhang L. 2016. Advances in hydrological modelling with the Budyko framework: a review. Prog Phys Geogr. 40(3):409–430.

Wang Q, Cheng L, Zhang L, Liu P, Qin S, Liu L, Jing Z. 2021. Quantifying the impacts of land-cover changes on global evapotranspiration based on the continuous remote sensing observations. J Hydrol. 598:126231.

Wigley BJ, Bond WJ, Hoffman MT. 2010. Thicket expansion in a South African savanna under divergent land use: local vs. global drivers? Glob Chang Biol. 16(3):964–976.

WWF-World Wide Fund for Nature. 2012. Miombo Eco-region "Home of the Zambezi" Conservation Strategy : 2011-2020. WWF-World Wide Fund For Nature. Harare. [accessed 2020 Dec 20]. Available from: https://www.searchworks.stanford.edu.

Yang X, Ren L, Liu Y, Jiao D, Jiang S. 2014. Hydrological response to land use and land cover changes in a sub-watershed of West Liaohe River Basin, China. J Arid Land. 6(6):678–689.

Yang G, Xue L, He X, Wang C, Long A. 2017. Change in land use and evapotranspiration in the Manas River Basin, China with long-term water-saving measures. Sci Rep. 7:1–11.

Yohannes H, Soromessa T, Argaw M, Dewan A. 2021a. Spatio-temporal changes in habitat quality and linkage with landscape characteristics in the Beressa watershed, Blue Nile basin of Ethiopian highlands. J Environ Manage. 281:111885.

Yohannes H, Soromessa T, Argaw M, Dewan A. 2021b. Impact of landscape pattern changes on hydrological ecosystem services in the Beressa watershed of the Blue Nile Basin in Ethiopia. Sci Total Environ. 793:148559

Yu D, Li X, Cao Q, Hao R, Qiao J. 2020. Impacts of climate variability and landscape pattern change on evapotranspiration in a grassland landscape mosaic. Hydrol Process. 34(4):1035–1051.

Zhang Y, Bi Z, Zhang X, Yu Y. 2019. Influence of landscape pattern changes on runoff and sediment in the Dali River watershed on the Loess Plateau of China. Land. 8(12):180.

Zhang L, Dawes WR, Walker GR. 2001. Response of mean annual ET to vegetation changes at catchment scale. Water Resour Res. 37(3):701–708.

Zhang M, Liu N, Harper R, Li Q, Liu K, Wei X, Ning D, Hou Y, Liu S. 2017. A global review on hydrological responses to forest change across multiple spatial scales: Importance of scale, climate, forest type and hydrological regime. J Hydrol. 546:44–59.

Zhang L, Hickel K, Dawes WR, Chiew FHS, Western AW, Briggs PR. 2004. A rational function approach for estimating mean annual evapotranspiration. Water Resour Res. 40(2):1–14.

Zhao M, Heinsch FA, Nemani RR, Running SW. 2005. Improvements of the MODIS terrestrial gross and net primary production global data set. Remote Sens Environ. 95(2):164–176.

Zhao Q, Wen Z, Chen S, Ding S, Zhang M. 2020. Quantifying land use/land cover and landscape pattern changes and impacts on ecosystem services. Int J Environ Res Public Health. 17:1–21.

Zhou G, Wei X, Chen X, Zhou P, Liu X, Xiao Y, Sun G, Scott DF, Zhou S, Han L, et al. 2015. Global pattern for the effect of climate and land cover on water yield. Nat Commun. 6:1–9.